IEEE Access
Multidisciplinary | Rapid Review | Open Access Journal

Received June 17, 2019, accepted June 30, 2019, date of publication July 4, 2019, date of current version December 27, 2019.

Digital Object Identifier 10.1109/ACCESS.2019.2926795

Low-Latency Oriented Network Planning for MEC-Enabled WDM-PON Based Fiber-Wireless Access Networks

XIN WANG, YUEFENG JI, JIAWEI ZHANG, LIN BAI, AND MIN ZHANG

State Key Laboratory of Information Photonics and Optical Communications, Beijing University of Posts and Telecommunications (BUPT), Beijing 100876, China

Corresponding author: Yuefeng Ji (jyf@bupt.edu.cn)

This work was supported by the National Nature Science Foundation of China Projects (No. 61771073, 61871051), and National Key R&D Program of China (No. SQ2018YFB180012-02).

ABSTRACT WDM-PON-based mobile edge computing (MEC)-enabled fiber wireless access networks (MFWAN) have been identified as a promising technology for next-generation broadband access. Low-latency oriented network planning of the WDM-PON-based MFWAN would be required for low-latency access to newly emerging latency-sensitive applications in the fifth-generation (5G) era. However, this would require a low-latency oriented network design in the network planning phase and has thus become a crucial challenge. In this paper, we investigate low-latency oriented network planning of the WDM-PON-based MFWAN under physical and management constraints. To this end, we develop a mathematical model to minimize total transmission latency for all latency-sensitive services. Our model is composed of the propagation latency on the paths and the processing latency on the network equipment and is subject to constraints of maximal transmission distance, maximal PON power budget, bandwidth requests, and the fronthaul latency limit under some functional split options. Given the model's complexity, we also propose a heuristic algorithm called latency-minimized integrated multi-associated positioning and routing algorithm (LMI-MAPRA). The simulation results show that the proposed algorithm outperforms the benchmark algorithm with more total transmission latency reductions in both sparse and dense networks. We also analyze the impact of key parameters on comparisons of different approaches in terms of low-latency optimal performances.

INDEX TERMS Technology planning, latency-sensitive application, network planning, WDM-PON, MEC-enabled access networks, FiWi networks.

I. INTRODUCTION

Future fifth generation (5G) networks will inspire different types of new applications, new network architectures, and new spectrum usages. Three typical application scenarios in 5G, e.g., eMBB (Enhanced Mobile Broadband), uRLLC (Ultra Reliable & Low Latency Communication) and mMTC (Massive Machine Type Communication), generate diverse network requirements such as low-latency, massive connectivity, high reliability and explosive growth of mobile bandwidth traffic [1]–[3] as shown in Fig. 1. With the emergence of 5G ultra-reliable and latency-sensitive applications, low latency is becoming one of critical requirements in 5G communications. Some of 5G latency-sensitive applications, e.g., self-driving cars, industrial interconnection and automation, require the end-to-end transmission latency be less than 5-10ms [4]–[7]. Therefore, it is necessary to consider the low-latency optimal design in the network planning phase.

Since data centers (DC) in the 4G era were commonly located far away from the end-subscribers [8], it was difficult to provide the availability and reachability of cloud services to achieve end-to-end low-latency communications. To mitigate such latency issue, a MEC concept is proposed to provide the reachable cloud computing capabilities (e.g., computing, storage, and caching) at the edge of access networks near subscribers [9], [10]. According to the network architecture evolution from 3GPP technical reports, the original two-level RAN composed of Base Band Unit (BBU) and Remote Radio Unit (RRU) in 4G is disaggregated into three level RAN composed of Central Unit (CU), Distributed Unit (DU), and Active Antenna Unit (AAU) in 5G [11]–[13].

The associate editor coordinating the review of this manuscript and approving it for publication was Cristina Rottondi.

FIGURE 1. New requirements for 5G.

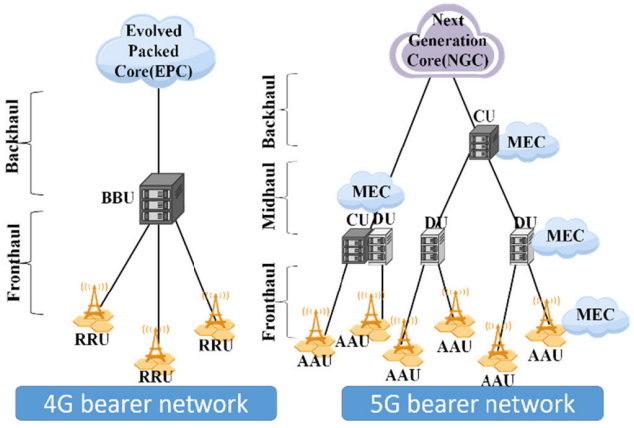

FIGURE 2. Illustration of the mobile bearer network architectures from 4G to 5G.

However, MEC-enabled three-level RAN could better support 5G low-latency communications than the original two-level RAN structures. Figure 2 illustrates the evolutions of the mobile bearer network architectures from 4G to 5G, taking into account all possible situations of the candidate locations of the MEC servers. In this study, we assume that the candidate locations of the MEC servers are only at the integration site of the CUDU co-located with the OLTs. On one side, from the perspective of the operators' concern of the real deployment cost, when the candidate locations of the MEC servers are at the AAU site, although the time delay is lowest, the deployment cost is high and the coverage is limited. On the other side, from the perspective of the low-latency communication requirement of the latency-sensitive services, CU and DU are considered to be at the same station so as to decrease the number of hops to achieve low-latency communications [14].

Recently, network convergence of ''optical plus radio'' has led to the development of future transport networks [15]. MEC-enabled Fiber-Wireless Access Network (MFWAN) [1] has emerged from combining advantages of high bandwidth and low latency of optical access technologies with characteristics of massive capacity, high flexibility and adaptability of future wireless networks [16], [17]. Since different broadband access network technologies can be flexibly selected in 5G transport networks, MFWAN is instrumental in realizing future 5G low-latency communications. However, the connection of CPRI signals in 5G transport networks with

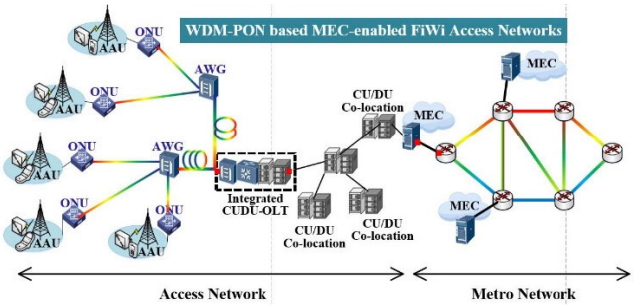

FIGURE 3. Illustration of the WDM-PON based MFWAN.

direct fiber or optical transport network (OTN) is too expensive [18], [19]. Passive optical networks (PON) are identified as a suitable technology to accelerate 5G network planning with flexible and cost-efficient access, and manageable networking control [20], [21]. In this paper, wavelength division multiplexing-PON (WDM-PON) is used as the bearer technology in the MFWAN. Figure 3 shows an illustration of WDM-PON based MFWAN, with MEC servers integrated at the edge of networks (which can be regarded as the access point of the edge of metropolitan network or RAN). Although the network architecture of WDM-PON based MFWAN provides many benefits, network planning of such a network architecture faces a critical challenge: how to establish an optimal topology for the WDM-PON based MFWAN with the goal of minimizing total transmission latency for all latency-sensitive applications.

To the best of our knowledge, most existing research on cost-effective network planning has been carried out for wired [22]–[24] or wireless networks [7], [11], [25], [26] with the goal of minimizing total deployment costs. In [22]–[24], cost-effective network planning models and algorithms were proposed for PON based smart grid networks and green field optical networks. Network planning of fronthaul [25], [26], backhaul and small-cell networks [7]–[11] over wireless networks suffers from more complexities than that of wire networks. To benefit from high bandwidth and ubiquitous access of optical and wireless technologies, hybrid fiber-wireless (FiWi) networks have been identified as a promising network architecture [32]–[34].

Most efforts to date have focused on minimizing total deployment cost (taking into account bandwidth requirements, delay budgets, complexity of radio remote head, maximum number of users per OLT and per wavelength, etc.). Some research [25], [29] has proposed network framework or mathematical models to optimize the infrastructure deployment costs. By considering all the factors just mentioned, a joint optimization framework was proposed to optimally deploy the entire 5G transport and wireless networks [25]. An optimization framework based on integer linear programming (ILP) was presented to plan cost-efficient PON deployments for small cell backhauling [29]. Other research [27], [28] tackled the problem with heuristic algorithms. A cost-effective backhaul was demonstrated to further

decrease the deployment cost in the sparse network scenarios [27]. In addition, a K-means clustering-based planning algorithm for the TWDM-PON based fiber backhaul network was proposed to minimize the dense deployment cost of 5G small cells [28]. For network planning of hybrid FiWi networks, an optimal network planning strategy was proposed, and optimal placement of virtualized BBU processing and multiple ONUs were also proposed [32]–[34]. In addition, a flexible and bandwidth-variable optical paths allocation between BBUs and RRUs were demonstrated in [35] by using SDN. The idea of the dynamic association between RRU and BBU enabled by a converged optical and wireless network is proposed in [36]. However, these approaches were carried out without stringent low-latency requirements, and cannot be applied to the MEC enabled hybrid FiWi access network. Considering the disadvantages of existing works, we discuss the network planning for WDM-PON based MEC-enabled Fiber Wireless Access Networks.

Our contributions and the differences from the previous works [7]–[36] of network planning over wireless or fiber-based networks are summarized as follows:

1) Our work is the first to investigate low-latency oriented network planning over MEC-enabled FiWi Access Networks while considering a) physical requirements of the latency limit in optical fronthaul networks under functional split options, maximal transmission distance and maximal power budget, and b) management consideration, and bandwidth requirements. Note that the fiber propagation latency is the main bottleneck of total transmission latency, which accounts for 70% of the end-to-end latency [37]. Hence, we will focus on how to minimize total transmission latency including the propagation latency along the paths and the processing latency on network equipments over the WDM-PON based MEC-enabled Fiber Wireless Access Networks for all latency-sensitive services at our best efforts.

2) This work pays more attention on the low-latency oriented network planning of both MEC-enabled centralized radio access networks and its optical fronthaul networks simultaneously during the network planning phase, while the previous works [7]–[36] mainly focused on the network planning of the mobile networks or its transport networks separately taking into no account of low-latency minimization.

To simplify the low-latency oriented network planning problem, we neglect the queuing latency at the ONU and other uncritical latency. In addition, a heuristic algorithm "LMI-MAPRA" is proposed to efficiently solve the mathematical model. The paper is organized as follows. In Section II, low-latency oriented network planning problem for WDM-PON based MFWAN is discussed, and a mathematical model is developed to formulate the problem. To solve the mathematical model efficiently, we propose a heuristic algorithm in Section III. Next, we conduct the simulation and analyze the results to evaluate the low-latency optimal performance of different approaches in Section IV. Lastly, Section V concludes the paper.

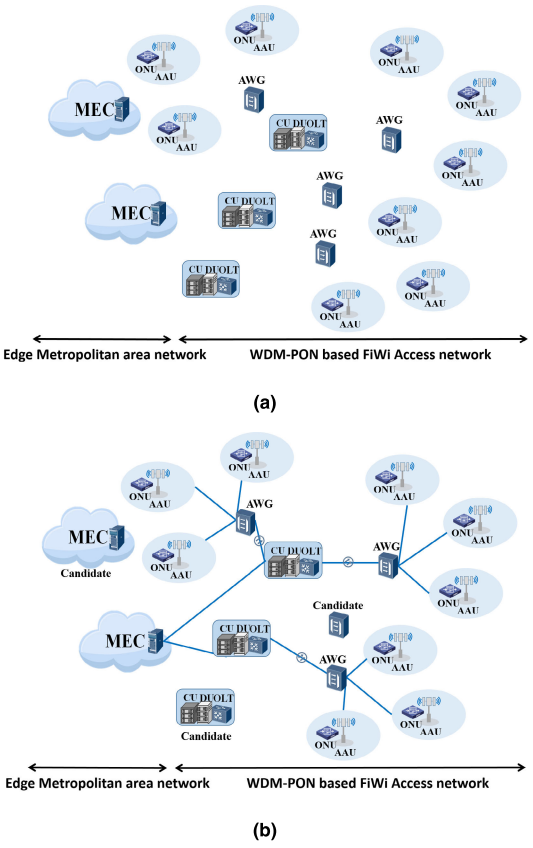

FIGURE 4. (a) The distributions of components and (b) the optimal connection topology of the exemplary representation of WDM-PON based MFWAN.

II. PROBLEM FORMULATION

A. LATENCY-MINIMIZED WDM-PON BASED MFWAN PLANNING

Figure 4 shows an exemplary representation of the WDM-PON based MFWAN. Note that we will consider candidate locations of MEC servers on the CU/DU sides between the metro area network and the access network. Given the sets of candidate positions of MEC servers, the CUDU co-located with OLT (CUDU-OLT), AWGs, and all positions of AAU co-located with ONU (AAU-ONU) as shown in Fig. 4 (a), our low-latency oriented WDM-PON based MFWAN planning problem is to find out the optimal configuration. Note that we assume that one ONU connects one AAU, which are co-located in the same station, meanwhile all ONUs are included in the PON system in this study. Some physical constraints, management considerations, and latency limits in the optical fronthaul network under some functional split options are also considered in the optimization process. In this paper, "the optimal configuration" indicates the connection plan with the minimal overall transmission latency from the AAUs to the MEC servers in order to guarantee the quality of services (QoS) in terms of low-latency for all the latency-sensitive services. The optimal planning processes include two main procedures, 1) identifying the optimal locations for candidate components of WDM PON-based MFWAN,

such as optimal locations of the AWGs, the CUDU-OLTs and the MEC servers; 2) identifying the optimal fiber routes that use the available fiber infrastructures among all identified components in the MFWAN. An exemplary representation of "the optimal configuration" in WDM-PON based MFWAN is illustrated in Fig. 4 (b). In the optimal planning topology, only one signal transmission path is available for each AAU-ONU from the AAU-ONU to one MEC server. All of the AAU-ONUs should be included in the optimal planning topology. However, other candidate components, e.g. AWGs, CUDU-OLTs and MEC servers, are not necessarily to be all connected to the optimal planning topology. Meanwhile, one AAU-ONU should be connected to one AWG, then through one CUDU-OLT to reach one MEC server.

The one-way transmission latency in MFWAN consists of the execution latency of the MEC server, the processing latency of CUDU-OLT, and the propagation latency on the fiber paths along one signal transmission path from one AAU-ONU to one MEC server, which can be written as

$$T = T_{mec} + T_{CUDU-OLT} + T_{fiber} \tag{1}$$

The execution latency for mobile device user i at the MEC server can be given as [34],

$$T_{mec} = t^{c}_{i,exe} = d_i / f^{c}_{i} \tag{2}$$

where d_i defines total number of CPU cycles to accomplish the computation task required by the i-th mobile device user, and f^{c}_{i} indicates the computation capability (CPU cycles per second) of the MEC server. To concentrate on low-latency oriented network planning over the MFWAN for all latency-sensitive services, f^{c}_{i} is considered as a constant for the computation task of each mobile device user. The time overhead for the MEC server to send the computation outcome back to the mobile device user or each AAU is neglected, since it is much smaller than the execution latency of computation input data. In addition, we assume that one AAU can only serve one type of latency sensitive services.

To concentrate on low-latency oriented network planning, the processing latency $T_{CUDU-OLT}$ at the CUDU-OLT for each AAU [39] is considered constant. The propagation latency, T_{fiber} is considered to be linear with the transmission distance. The propagation latency of the fiber $l_{i,j}$ per kilometer is η.

$$T_{fiber} = l_{i,j} \cdot \eta \tag{3}$$

Since the propagation latency and the processing latency are the main bottleneck of the total transmission latency [37], the queuing latency and other uncritical latency are neglected. In this study, the propagation latency on fiber cables along the paths and the processing latency of the MEC server and the CUDU-OLT are considered in the transmission latency.

In addition, low-latency oriented network planning over the MFWAN should consider some constraints, such as:

1) physical requirement of low-latency oriented network planning

- latency limit in the optical fronthaul network under some split options, which we set to 100 μs.
- maximum end-to-end transmission distance.
- maximum power budget from the AAU-ONU to the CUDU-OLT, which includes the launch power of the transmitter, receiver sensitivity, the loss power of the splitter insertion, the power attenuation on the fiber link, etc.

2) management consideration

- constraint of the maximal number of wavelength λ per AWG.
- each AAU-ONU should be connected to one AWG.
- one available signal transmission path is provided from the MEC server through one CUDU-OLT and one AWG to each AAU-ONU.
- constraint of the MEC server number that are turned on.
- bandwidth requirement of all latency-sensitive services at the AAU-ONUs under some split options.

B. MATHEMATICAL MODEL

In this section, we propose a mathematical model for the low-latency oriented network planning problems for the latency-sensitive services over the WDM-PON based MFWAN. We first define the notation of network parameters and variables, then we describe the objective function and the constraints of the mathematical formulation for the low-latency oriented network planning problem.

1) NETWORK PARAMETERS

Several network parameters need to be defined:

- M_{mec}: The set of potential positions of MEC servers, where N_{mec} is the total number of M_{mec}, and the element of M_{mec} is indicated as m.
- C_{CUDU}: The set of potential positions of the integration site of the CUDU and the OLT, where N_{CUDU} is the total number of C_{CUDU}, and the element of C_{CUDU} is indicated as c.
- S_{AWG}: The set of the potential positions of AWGs, where N_{AWG} is the total number of S_{AWG}, and each element of S_{AWG} is indicated as s.
- A_{ONU}: The set of all the positions of the ONUs, where N_{ONU} is the total number of A_{ONU}, and the element of A_{ONU} is indicated as a.
- W: The distance matric of the physical topology for the WDM-PON based MFWAN, which is indicated as $\mathrm{W} = \{w_{ij}$.
- l^{total}_{ij}: The total distance between the i^{th} node and the j^{th} node in the W.
- P^{total}_{ij}: The total power budget from the i^{th} CUDU-OLT node to the j^{th} AAU-ONU node in W, including the launch power of the OLT, the loss power of the AWG insertion, the ONU sensitivity and the fiber loss power per kilometer.
- PB: The power budget of the PON, which is set to 21dBm.

- Pl: The launch power of the OLT-PON, which is set to +3dBm.
- P_{os}: The receiving sensitivity of the ONU optical port, which is set to −20dBm.
- AF: The fiber loss power per kilometer with 1310nm wavelength fiber cable under normal conditions, which is set to 0.35dBm/km.
- AS: The loss power of the AWG insertion, which is set to 10dBm.
- Δs: The maximum wavelength number of the AWG output ports.
- ST: The set of the AWG types, where $S_t \in \{1{:}4, 1{:}8, 1{:}16, 1{:}32\}$.
- T_{mec}: The processing latency of one MEC server.
- T_{CUDU}: The processing latency of one CUDU-OLT.
- η: The fiber propagation latency per kilometers, which is set to $5\mu s/km$.
- T_{FON}: The maximum transmission latency in the optical fronthaul network, which is set to $100\mu s$.
- B: The carrier bandwidth of one AAU, which is set to 100MHz.
- L_a: The proportion of occupied traffic load of the a-th AAU, where $L_a \in [0.1, 1]$.
- A: The number of antennas for one AAU, which we set to 4.
- $BMEC_{up}$: The maximum bandwidth capacity for upstream from the CUDU-OLT to the MEC server, which we set to 100 Gb/s.
- $BMEC_{down}$: The maximum bandwidth capacity for downstream from the MEC server to the CUDU-OLT, which we set to 100 Gb/s.
- $BU1_a$: The transport bandwidth for upstream of the a^{th} AAU using the split option 7, where $\mathrm{BU1_a} = 2.432 \cdot B \cdot A \cdot L_a/1000$.
- $BD1_a$: The transport bandwidth for downstream of the a^{th} AAU using the split option 7, where $\mathrm{BD_a} = 7.493 \cdot B \cdot A \cdot L_a/1000$.
- L_{max}: The maximum end-to-end transmission distance from one AAU to one MEC server.

2) VARIABLES

The binary and integer decision variables in the optimization model are indicated as follows.

- $\sigma^a_{m,c}$ is a binary variable, which represents the connection status between the m^{th} MEC server and the c^{th} CUDU-OLT for each a^{th} AAU-ONU, where $\mathrm{m} \in M_{mec}, c \in C_{CUDU}, and A \in A_{ONU}$. If $\sigma^a_{m,c} = 1$, the m^{th} MEC server is connected to c^{th} CUDU-OLT for each a^{th} AAU-ONU; otherwise, $\sigma^a_{m,c} = 0$.
- $\sigma^a_{c,s}$ is a binary variable, which represents the connection status between the c^{th} CUDU-OLT and s^{th} AWG for each a^{th} AAU-ONU, where $c \in C_{CUDU}$, $\mathrm{s} \in S_{AWG}$, and $A \in A_{ONU}$. If $\sigma^a_{c,s} = 1$, the c^{th} CUDU-OLT is connected to s^{th} AWG for each a^{th} AAU-ONU; otherwise, $\sigma^a_{c,s} = 0$.
- $\sigma_{s,a}$ is a binary variable, which represents the connection status between the s^{th} AWG and a^{th} AAU-ONU, where $\mathrm{s} \in S_{AWG}, andA \in A_{ONU}$. If $\sigma_{s,a} = 1$, the s^{th} AWG is connected to the a^{th} AAU-ONU; otherwise, $\sigma_{s,a} = 0$.
- λ_m is a binary variable, which represents the utilization status of the m^{th} MEC server, where $\mathrm{m} \in M_{mec}$. If $\lambda_m = 1$, the m^{th} MEC server is used; otherwise, $\lambda_m = 0$.

The total transmission latency contains several parts: the processing latencies of the MEC servers and the CUDU-OLTs, and the propagation latency of the fiber links along the paths. The objective function shown in Eq. (4) is subject to some constraints, shown in Eqs. (5)-(14). The first three items in Eq. (4) indicate the propagation latency on the fiber links of the optimal connection among the MEC servers, CUDU-OLTs, AWGs and AAU-ONUs. The last two items indicate the processing latency of the identified MEC servers and CUDU-OLTs.

- Objective:

Minimize

$$\sum_{\substack{s\in S_{AWG}\\ a\in A_{ONU}}} \sigma_{s,a}\cdot w_{s,a}\cdot\eta + \sum_{\substack{c\in C_{CUDU}\\ s\in S_{AWG}\\ a\in A_{ONU}}} \sigma^a_{c,s}\cdot w_{c,s}\cdot\eta + \sum_{\substack{m\in M_{mec}\\ c\in C_{CUDU}\\ a\in A_{ONU}}} \sigma^a_{m,c}\cdot w_{m,c}\cdot\eta + \sum_{\substack{m\in M_{mec}\\ c\in C_{CUDU}\\ a\in A_{ONU}}} \sigma^a_{m,c}\cdot T_{mec} + \sum_{\substack{m\in M_{mec}\\ c\in C_{CUDU}\\ a\in A_{ONU}}} \sigma^a_{m,c}\cdot T_{CUDU-OLT} \tag{4}$$

- Under constraints

$$\sum_{c\in C_{CUDU}} \sigma^a_{c,s} = \sigma_{s,a}, \quad \forall a \in A_{ONU},\ \forall s \in S_{AWG} \tag{5}$$

$$\sum_{m\in M_{mec}} \sigma^a_{m,c} = \sum_{s\in S_{AWG}} \sigma^a_{c,s}, \quad \forall c \in C_{CUDU},\ \forall a \in A_{ONU} \tag{6}$$

$$\sum_{s\in S_{AWG}} \sigma_{s,a} = 1, \quad \forall a \in A_{ONU} \tag{7}$$

Equations (5)-(7) guarantee that only one signal transmission path is available from each AAU-ONU to one MEC server for one AAU. Equation (5) ensures that each AAU should connect to one CUDU-OLT through one AWG. Equation (6) ensures that each AAU can require the edge computing from one MEC server. Equation (7) guarantees that one AAU can only connect one AWG output port.

$$1/\sum_{a\in A_{ONU}} \sigma_{s,a} \geq \Delta s, \forall s \in S_{AWG} \tag{8}$$

The constraint of the AWG split ratio is formulated as Eq. (8), which indicates that the maximal number of the AAU-ONUs connected to one AWG should be less than the

maximum number of the AWG output ports.

$$\lambda_m \leq \sum_{\substack{c\in C_{CUDU}\\ a\in A_{ONU}}} \sigma^a_{m,c} \leq \lambda_m \cdot N_{CUDU}, \quad \forall m \in M_{MEC} \tag{9}$$

Equation (9) guarantees at least one MEC server is in use, and the maximum number of MEC servers that are turned on should be less than the total number of the MEC servers.

$$\sum_{s\in S_{AWG}} \sigma_{s,a} \cdot w_{s,a} \cdot \eta + \sum_{s\in S_{AWG}} \sigma^a_{c,s} \cdot w_{c,s} \cdot \eta \leq T_{FON}, \quad \forall a \in A_{ONU}, \forall c \in C_{CUDU} \tag{10}$$

The latency constraint in the optical fronthaul network under split options is formulated as Eq. (10).

$$\sum_{\substack{c\in CUDU\\ a\in A_{ONU}}} BU1_a \cdot \sigma^a_{m,c} \leq BMEC_{up}, \quad \forall m \in M_{mec} \tag{11}$$

$$\sum_{\substack{c\in CUDU\\ a\in A_{ONU}}} BD1_a \cdot \sigma^a_{m,c} \leq BMEC_{down}, \quad \forall m \in M_{mec} \tag{12}$$

The constraint of the bandwidth capacity is formulated as Eqs. (11)-(12). Equation (11) guarantees the constraint of the transport bandwidth for upstream from the CUDU-OLT to the MEC server for the a-th AAU using the split option 7. Equation (12) guarantees the constraint of the transport bandwidth for downstream from the MEC server to the CUDU-OLT for the a-th AAU using the split option 7.

$$l^{total}_{ij} = \sum_{c\in C_{CUDU}} \sigma^a_{m,c} \cdot w_{m,c} + \sum_{\substack{c\in C_{CUDU}\\ s\in S_{AWG}}} \sigma^a_{c,s} \cdot w_{c,s} + \sum_{s\in S_{AWG}} \sigma_{s,a} \cdot w_{s,a} \leq L_{\max}, \quad \forall m \in M_{mec}, \forall a \in A_{ONU} \tag{13}$$

$$P^{total}_{ij} = \sum_{s\in S_{AWG}} \sigma_{s,a} \cdot w_{s,a} \cdot AF + \sum_{s_t\in ST} s_t \cdot AS + \sum_{s\in S_{AWG}} \sigma^a_{c,s} \cdot w_{c,s} \cdot AF \geq P_{ONU} + P_L - P_B, \quad \forall a \in A_{ONU}, \forall c \in C_{CUDU} \tag{14}$$

The physical constraints of the respective maximal transmission distance and maximal power budget are guaranteed in Eqs. (13) and (14).

III. PROPOSED HEURISTIC ALGORITHMS

Although the mathematical model solved by the CPLEX solver can provide the optimal solution for the low-latency oriented network planning problems under certain conditions, it increases time complexity and memory resources for large-scale mixed integer linear programming problems [25], [27]. Moreover, network planning for a large-scale network cannot be solved by the mathematical model efficiently. To solve this problem, a heuristic algorithm, called "Latency-Minimized Integrated Multi-associated Positioning and Routing algorithm" (LMI-MAPRA), is proposed. In addition, a benchmark algorithm is also introduced. The detailed processes of the proposed LMI-MAPRA and the benchmark algorithm are discussed as follows.

A. PROPOSED ALGORITHM

Table 1 illustrates the pseudo-code of the proposed algorithm LMI-MAPRA, and the detailed procedures are as follows.

Step 1: Given the sets of the candidate positions of the MEC servers, M_{mec} = {m, the candidate positions of the CUDU-OLTs, C_{CUDU} ={c}, and the candidate positions of the AWGs, S_{AWG} = {s; all of the AAU-ONUs, A_{ONU} = {a;

Step 2: Initialize the optimal connection topology of MFWAN, $\mathcal{T}$; and total transmission latency of all latency-sensitive services, T;

Step 3: Classify and mark all different types of nodes in $W(V, E)$;

Step 4: To establish the optimal configuration connection topology of the MFWAN, we first configure the optimal connection between $a \in A_{ONU}$ and $s \in S_{AWG}$, under the constraints of the AWG split ratio in Eq. (8);

Step 5: According to the connection principle between $a \in A_{ONU}$ and $s \in S_{AWG}$, to connect all AAU-ONUs to the candidate AWGs, while satisfying the constraint of Eq. (7) that one AAU can only connect one AWG output port;

Step 6: Initialize the path storage set P and the transmission latency storage set T;

Step 7: Apply the "Warshall-Floyd" algorithm [42] to establish the optimal configuration connection between $a \in A_{ONU}$ and $s \in S_{AWG}$;

Step 8: Obtain the path $\mathcal{T} \leftarrow P_{a,s}$ with minimal transmission latency of T for the node pair (a$\rightarrow s$); the connected AWG set of W_S is also obtained;

Step 9: According to the connection principle of Eq. (5), to connect all AWGs in W_S to all candidate CUDU-OLTs in C_{CUDU};

Step 10: Apply the "Warshall-Floyd" algorithm [42] to establish the optimal configuration connection between $s \in W_S$ and $c \in C_{CUDU}$;

Step 11: Obtain the path $\mathcal{T} \leftarrow P_{s,c}$ with the minimal transmission latency of T for the node pair (s$\rightarrow c$); the connected CUDU-OLT set of W_{CUDU} is also obtained;

Step 12: Repeat from step 4 to step 11 until the fronthaul latency constraint of Eq. (10) and the maximal power budget of Eq. (14) are satisfied;

Step 13: According to the connection principle of Eq. (5), if the constraint of the number of MEC servers that are turned on, formulated as Eq. (9), is satisfied;

Step 14: To configure the optimal connection between all connected CUDU-OLTs in W_{CUDU} and all candidate MEC servers in M_{mec};

Step 15: Initialize the path storage set P and the transmission latency storage set T;

Step 16: Apply the "Warshall-Floyd" algorithm [42] to establish the optimal configuration connection between $c \in W_{CUDU}$ and $m \in M_{mec}$, while satisfying the constraints of Eq. (11) and Eq. (12) that the transport bandwidth capacity for the respective upstream and downstream between the

TABLE 1. The pseudo-code of proposed algorithm LMI-MAPRA.

Algorithm 1: Latency-Minimized Integrated Multi-associated Positioning and Routing algorithm (LMI-MAPRA).

Input: Candidate positions of the MEC servers, the CUDU-OLTs , and the AWGs; all positions of the AAU-ONUs; distance matrix W(V, E).
Output: The optimal connection topology of the MFWAN $\urcorner$; and total transmission latency of all latency-sensitive services, indicated as T.

1. Classify and mark all different types of nodes in $W(V, E)$;
2. **while** the AWG split ratio constraint of Eq. (8) is satisfied **do**
3. According to the connection principle of Eq. (7);
4. **for** all $a \in A_{ONU}$ **do**
5. Initialize the path storage set P and the transmission latency storage set T;
6. **for** candidate $s \in S_{AWG}$ **do**
7. Apply the "Warshall-Floyd" algorithm [42] to establish the optimal configuration connection between $a \in A_{ONU}$ and $s \in S_{AWG}$;
8. obtain the path $\urcorner \leftarrow P_{a,s}$ with minimal T for (a→ s);
9. **end if end for end for end while**
10. obtain the connected AWG set of W_S;
11. According to the connection principle of Eq. (5);
12. **for** all connected candidate AWG $s \in W_S$ **do**;
13. Initialize the path storage set P and the transmission latency storage set T;
14. **for** all candidate CUDU-OLT $c \in C_{CUDU}$ **do**
15. Apply the "Warshall-Floyd" algorithm [42] to establish the optimal configuration connection between $s \in W_S$ and $c \in C_{CUDU}$;
16. obtain the path $\urcorner \leftarrow P_{s,c}$ with minimal T for (s→ c);
17. **end for end for**
18. Repeat from step 2 to 17 until the fronthaul latency constraint of Eq. (10) and the maximal power budget of Eq. (14) are satisfied;
19. Obtain the connected CUDU-OLT set of W_{CUDU};
20. **while** the constraint of the number of MEC servers that are turned on, Eq. (9) is satisfied **do**
21. According to the connection principle of Eq. (6);
22. **for** all $c \in W_{CUDU}$ **do**
23. Initialize the path storage set P and the transmission latency storage set T;
24. **for** all candidate $m \in M_{mec}$ **do**
25. **if** the transport bandwidth capacity for the respective upstream and downstream between the MEC servers and the CUDU-OLTs of the a-th AAU using the split option 7, shown in Eq. (11) and Eq. (12), are satisfied **do**
26. Apply the "Warshall-Floyd" algorithm [42] to establish the optimal configuration connection between $c \in W_{CUDU}$ and $m \in M_{mec}$;
27. obtain the path $\urcorner \leftarrow P_{c,m}$ with minimal T for (c→ m);
28. **end if end for end for end while**
29. Repeat from step 18 to 28 until the maximal distance constraint of Eq. (13) is satisfied;
30. Calculating total transmission latency of all services;

return $\urcorner$ and T;

MEC servers and the CUDU-OLTs for the a-th AAU using the split option 7;

Step 17: Obtain the path $\urcorner \leftarrow P_{c,m}$ with the minimal transmission latency of T for the node pair (c→m);

Step 18: Repeat from step 12 to step 17 until the maximal distance constraint of Eq. (13) is satisfied;

Step 19: Calculating total transmission latency of all services, saved as T;

Step 20: Return the optimal configuration connection topology of $\urcorner$ and the total transmission latency of T;

TABLE 2. The pseudo-code of benchmark algorithm.

Algorithm 2: Partial Sampling Enumeration Approach (PSEA).

Input: Candidate positions of the MEC servers, the CUDU-OLTs, and the AWGs; all positions of the AAU-ONUs; distance matrix W(V, E).
Output: The connection topology of MFWAN, $\urcorner$, and total transmission latency, T.

1. Classify and mark the nodes of different types in $W(V, E)$;
2. **while** the optimal configuration connection topology is satisfied with the constraints of Eq. (5) and Eq. (6) among M_{mec}, C_{CUDU}, S_{AWG}, and A_{ONU}, and the constraints of maximal end-to-end transmission distance in Eq. (13) and maximal end-to-end power loss in Eq. (14) **do**
3. **for** all node positions in the physical topology of PEAN **do**
4. Traverse all the possible end-to-end paths;
5. for each (a→ s) node pair, $a \in A_{ONU}$ *and* $s \in S_{AWG}$, considering the constraints of Eq. (7) and (8);
6. for each (s→ c) node pair, $s \in S_{AWG}$ *and* $c \in C_{CUDU}$, considering the fronthaul latency limit of Eq. (10);
7. for each (c→ m) node pair, $c \in C_{CUDU}$ *and* $m \in M_{mec}$, considering the constraints of the number of MEC servers that are turned on of Eq.(9), and the transport bandwidth constraints for the respective upstream and downstream between $c \in C_{CUDU}$ *and* $m \in M_{mec}$ using the split option 7, shown in Eq. (11) and Eq. (12);
8. Select K (1<K<|V|/2) number of the traversed constrained end-to-end paths randomly;
9. Apply the "Warshall-Floyd" algorithm [42] to establish the optimal configuration connection;
10. $\urcorner \leftarrow$ {v};$\urcorner \leftarrow$ {e};
11. obtain the path $P_{a,s}$ with minimal T for (a→ s), the path $P_{s,c}$ with minimal T for (s→ c), and the path $P_{c,m}$ with minimal T for (c→ m);
12. **end**
13. **end**

return $\urcorner$ and T;

B. BENCHMARK ALGORITHM

In order to evaluate the performance of the proposed algorithm, the constrained enumeration approach is chosen as the benchmark algorithm [22]. To compare different approaches in the same situation, the enumeration approach, which is called as "Partial Sampling Enumeration Approach (PSEA)," considers the same constrains as the proposed algorithm. Table 2 illustrates the pseudo-code of benchmark algorithm PSEA. K numbers of end-to-end paths are selected from all paths among the MEC servers, CUDU-OLTs, AWGs, and AAU- ONUs. Then, under the constraints of Eqs. (5)-(14), the optimal configuration connection topology$\urcorner$with minimal transmission latency for all services is obtained, as shown from line 3 to line 12.

C. TIME COMPLEXITY ANALYSIS

Based on the detailed procedures of different approaches above, the time complexity of different algorithms is analyzed as follows. The overall time complexity of the proposed algorithm is $O(n^2)$, and the overall time complexity of the benchmark algorithm is $O(n^3)$.

IV. SIMULATION RESULTS AND ANALYSIS

To evaluate the latency-minimized performance of the proposed approaches, we simulate and compare different approaches with the CPLEX linear programming solver and

the MATLAB [25]. We consider two tested networks of both sparse and dense network scenarios, where candidate network components of the MFWAN are randomly distributed in the network range of $20 \times 20\text{km}^2$. In addition, we consider a WDM-PON that supports up to 100 Gb/s bandwidth capacity for the respective upstream and downstream between the CUDU-OLTs and the MEC servers in the simulation. The maximal bandwidth of a single wavelength of WDM-PON is set to 10 Gb/s.

For computation tasks of mobile devices, the application in [40] is considered, where the data size for a computation task is set to 100 KB and the total number of CPU cycles d_i is set to 2 Megacycles. The computational capability for a mobile device user i is indicated as $f_i^c = 10$ GHz [41]. To focus on the low-latency oriented network planning problem, T_{MEC} and $T_{CUDU-OLT}$ are considered constant and set to 40μs. For the management parameters, the maximal end-to-end transmission distance is set to 20km, and the propagation latency η per kilometer of the fiber cable is held constant at $5\mu s/km$. The PON power budget is set to 21dBm, and the respective launch power of OLT and the ONU sensitivity are set to $+3$dBm and -20dBm. In the simulation, the split ratio of the AWG is offset to 1:16, and its power loss is 10dBm. The fiber loss power per kilometer is set to -0.35dBm/km. The carrier bandwidth of the base station is set to 100 MHz with 16QAM for upstream, and the number of antennas is set to 4.

A. COMPARISON OF DIFFERENT APPROACHES

1) COMPARISON WITH INCREASE OF DIFFERENT PARAMETERS

To compare the performance of different approaches, we simulated this on both sparse and dense networks as different parameters increase, such as the AAU number and traffic load of AAUs. Note that we assume one AAU connects to one ONU, and each ONU is allocated with one single wavelength. The network components are randomly distributed in the sparse and dense networks of 20×20 km^2. In the sparse network, there are two MEC servers, four CUDU-OLTs and four AWGs, and the AAU number increases from 4 to 20 with an interval of 2. In the dense networks, there are 12 MEC servers, 24 CUDU-OLTs and 24 AWGs, and the AAU number increases from 26 to 42 with an interval of 2. We assume that one AAU can only serve one type of latency-sensitive services. As the AAU number increases, the comparison results of approaches for both sparse and dense networks are shown in Fig. 5 (a) and Fig. 5 (b). As the number of AAUs increases in both network scenarios, we observe that the proposed algorithm outperforms the benchmark algorithm with less transmission latency in providing all services. Specifically, results calculated by the proposed algorithm "LMI-MAPRA" are close to the optimal solution of the mathematical model in the sparse network scenario. The proposed algorithm outperforms the benchmark algorithm significantly in terms of low-latency optimal performance in dense networks as shown in Fig. 5 (b).

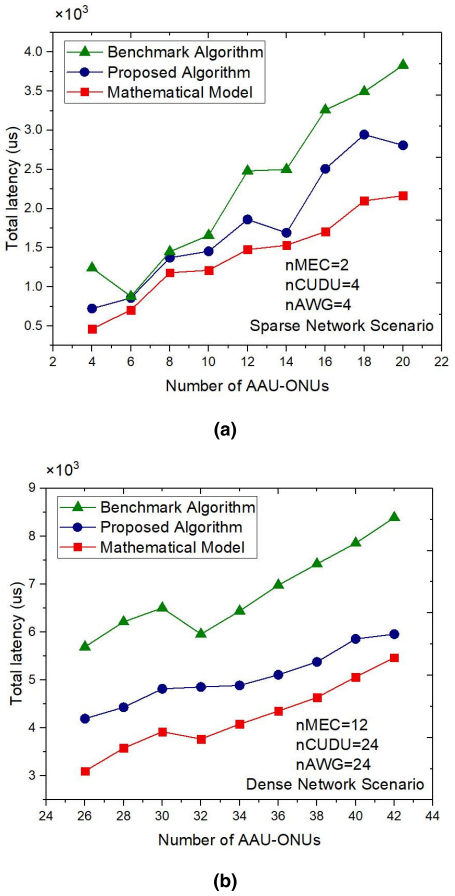

FIGURE 5. Comparison of approaches on latency-minimized performance as the AAU number increases in (a) sparse network scenario and (b) dense network scenario.

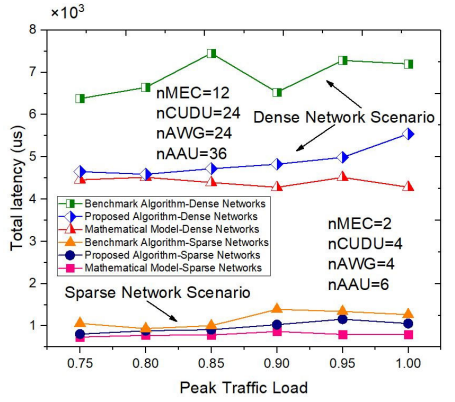

FIGURE 6. Comparison of approaches on the latency-minimized performance as the traffic load of AAU increases in both sparse and dense network scenarios.

As the peak traffic load of AAU-ONUs increases, the comparison of approaches on latency-minimized performances are also conducted for both sparse and dense networks as shown in Fig. 6. The peak traffic load $\alpha(0.1 \leq \alpha \leq 1)$ means the maximum value of the traffic loads in a certain interval of $[0.1,\alpha]$. The simulation results show that as the peak traffic load increases from 0.75 to 1 with an interval

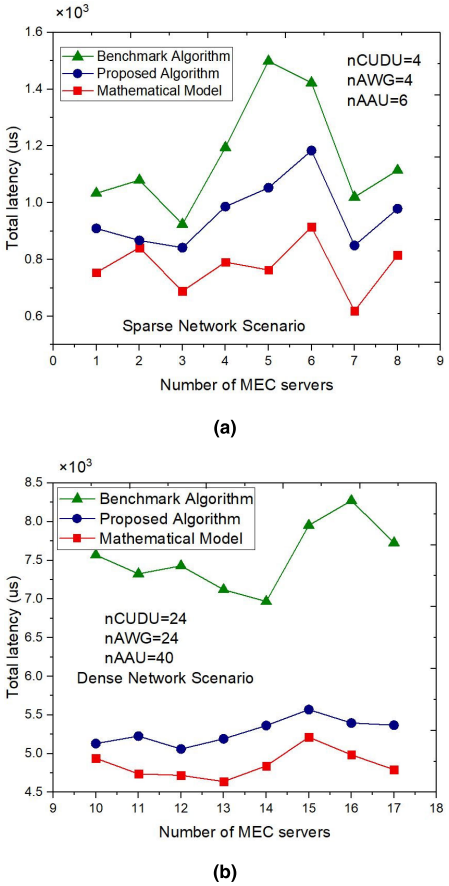

FIGURE 7. Impact of the MEC number on approach comparisons of latency-minimized performance in (a) sparse network scenario and (b) dense network scenario.

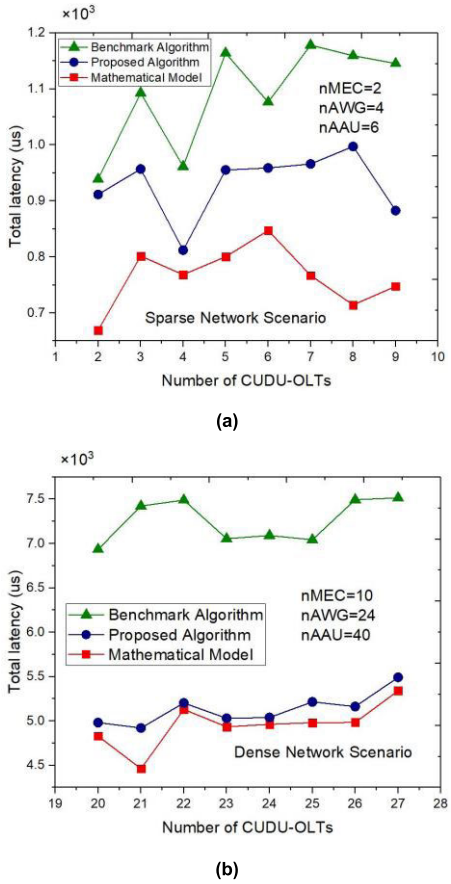

FIGURE 8. Impact of the CUDU-OLT number on different approach comparisons of the latency-minimized performance in (a) sparse network scenario and (b) dense network scenario.

of 0.05, the proposed algorithm shows better performances on total transmission latency reductions for all services as compared with the benchmark algorithm in both sparse and dense networks. We also observe that LMI-MAPRA outperforms the benchmark algorithm obviously in terms of total latency reductions in the dense network. This is reasonable because the proposed algorithm LMI-MAPRA searches the optimal configuration connection among all candidate components at best efforts efficiently rather than selects the solution in the local range with the benchmark algorithm. Therefore, it is reasonable that LMI-MAPRA consumes less transmission latencies and is close to the results of the mathematical model.

As the respective AAU number and the peak traffic load increases, the proposed algorithm outperforms the benchmark algorithm in terms of low-latency optimizing performances. Such performance advantages are especially more significant in dense network scenarios.

2) IMPACT OF THE MEC NUMBER

We also evaluate the impact of the MEC number on comparisons of different approaches in the tested sparse and dense network scenarios as shown in Fig. 7 (a) and 7 (b), respectively. In the sparse network, there are four CUDU-OLTs, four AWGs, six AAU-ONUs and the number of MEC servers increases from 1 to 8 with an interval of 1. In the dense network, there are 24 CUDU-OLTs, 24 AWGs, 40 AAU-ONUs and the number of MEC servers increases from 10 to 17 with an interval of 1. As the number of MEC servers increases, the proposed algorithm outperforms the benchmark algorithm consuming less total transmission latencies. Specifically, the proposed algorithm outperforms the benchmark algorithm significantly and is close to the optimal solution calculated by the mathematical model in the dense networks. Therefore, the MEC number shows no obvious impact on performance comparisons of approaches in the simulation of this study.

3) IMPACT OF THE CUDU-OLT NUMBER

We also evaluate the impact of the CUDU-OLT number on performance comparisons of approaches in different network scenarios. In the sparse network of Fig. 8 (a), there are two MEC servers, four AWGs, six AAU-ONUs, and the number of CUDU-OLTs increases from 2 to 9 with an interval of 1. In the dense network of Fig. 8 (b), there are 10 MEC servers, 24 AWGs, 40 AAU-ONUs, and the CUDU-OLT number increases from 20 to 27 with an interval of 1.

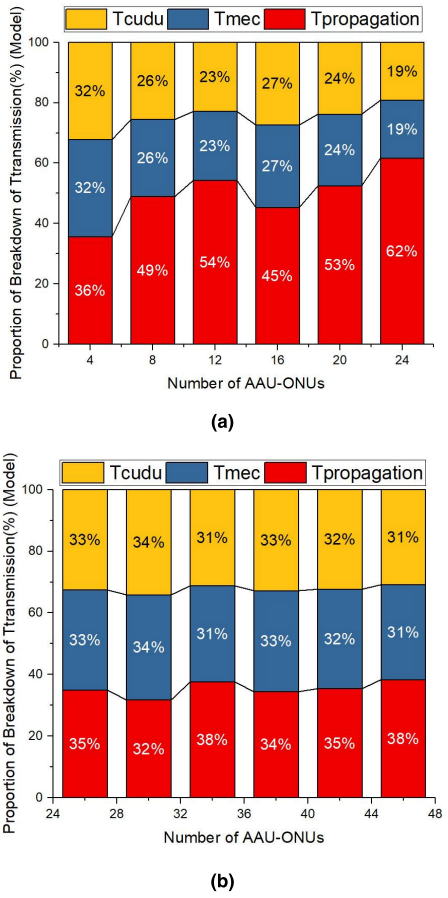

FIGURE 9. Proportion of Breakdown of total transmission latency with the mathematical model in (a) sparse network scenario and (b) dense network scenario.

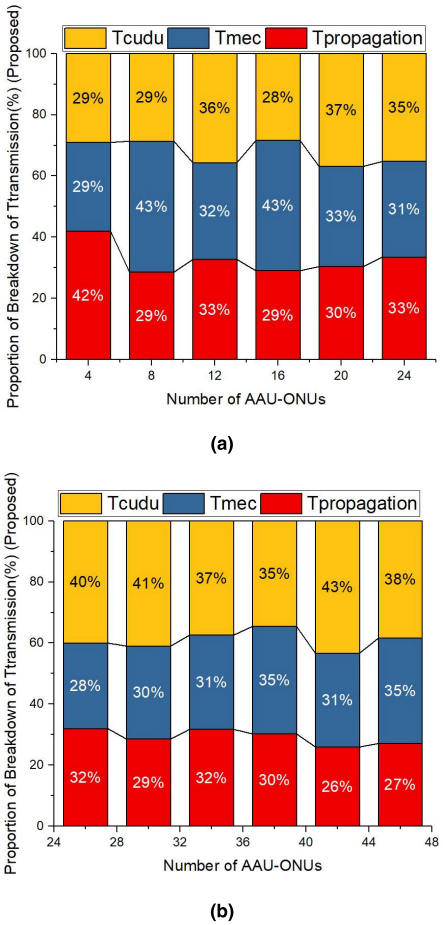

FIGURE 10. Proportion of Breakdown of total transmission latency with the proposed algorithm in (a) sparse network scenario and (b) dense network scenario.

As the CUDU-OLT number increases, the simulation results show that total transmission latency obtained by the proposed algorithm is less than that obtained by the benchmark algorithm. Specifically, proposed algorithm reaches near-optimal results of the mathematical model and gives significant improvement on the latency-minimized performance, compared with the benchmark algorithm in the dense network scenarios as shown in Fig. 8 (b). Therefore, the increase of the CUDU-OLT number shows no significant impact on the comparison of different approaches.

4) BREAKDOWN OF TOTAL TRANSMISSION LATENCY

We simulated the mathematical model and the proposed algorithm for both sparse and dense tested networks scenarios, aiming to evaluate which part is dominant in the total transmission latency as shown in respective Fig. 9 and Fig.10. In this study, total transmission latency includes three major parts, i.e., the propagation latency along the fiber paths, the execution latency of the MEC servers, and the processing latency of the CUDU-OLTs. In the sparse networks as shown in Fig. 9 (a) and 10 (a), there are two MEC servers, four CUDU-OLTs, four AWGs, and the number of AAU-ONUs increases from 4 to 24 with an interval of 4. In the dense networks as shown in Fig. 9 (b) and Fig. 10 (b), there are 12 MEC servers, 24 AWGs, 24 CUDU-OLTs, and the number of AAU-ONUs increases from 26 to 46 with an interval of 4.

From the simulation results as shown in Fig. 9, we observe that the propagation latency occupies by respective 49.83% and 35.33% of total transmission latency in average in the sparse and dense networks. Thus, the propagation latency shows a dominant part in total transmission latency obtained by the mathematical model over most of network scenarios. Moreover, from the simulation results obtained by the proposed algorithm as shown in Fig. 10 (a), the processing latency of the MEC servers occupies by 35.17% of total transmission latency, and shows a dominant part in total transmission latency with the proposed algorithm in sparse network scenario. However, the processing latency of the CUDU-OLTs occupies by 39% of total transmission latency, and presents a dominant part in total transmission latency obtained by the proposed algorithm in dense network scenario as shown in Fig. 10 (b). Therefore, from the simulation results, there is no typical law to present which part, i.e., the propagation latency, the execution latency of the MEC servers, and the processing latency of the CUDU-OLTs, plays a dominant role in the total transmission latency.

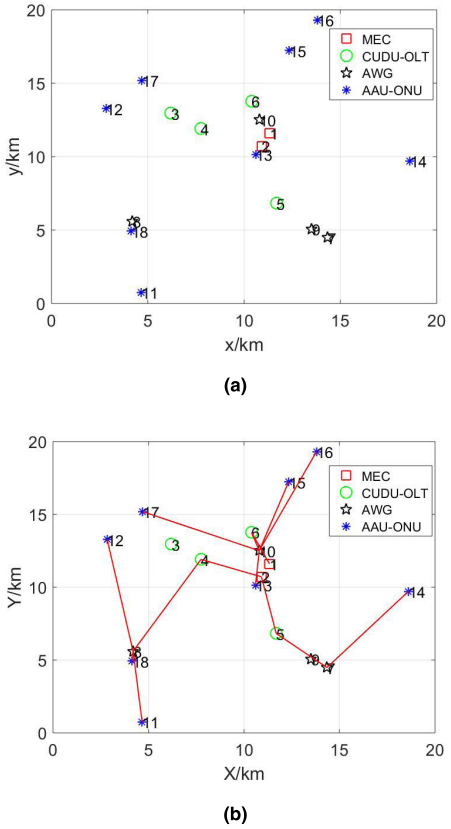

FIGURE 11. The application results of the proposed algorithm in sparse network scenario, which (a) the distribution of network devices in the MEC-enabled WDM-PON based FiWi Access Network, (b) the optimal planning topology of the proposed algorithm.

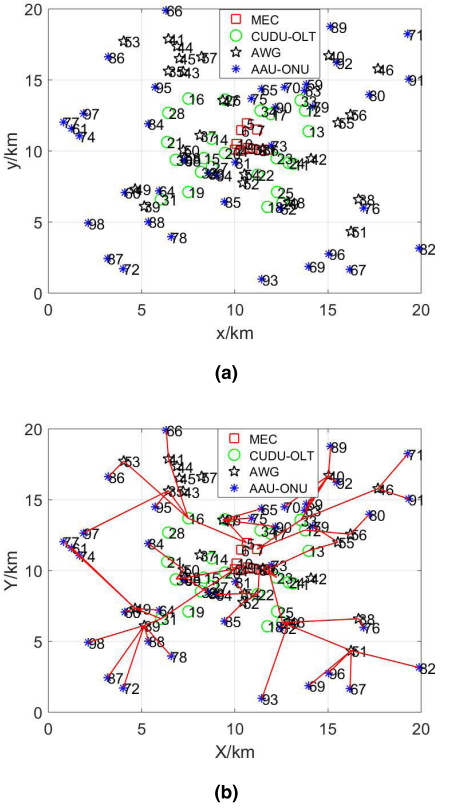

FIGURE 12. The application results of the proposed algorithm in dense network scenario, which (a) the distribution of network devices in the MEC-enabled WDM-PON based FiWi access network, (b) the optimal planning topology of the proposed algorithm.

TABLE 3. The simulation parameters set up.

Network scenario	Sparse network	Dense network
nMEC	2	10
nCUDU	4	24
nAWG	4	24
nAAU	8	40
Traffic Load	Randomly[0.1,1]	Randomly[0.1,1]
Network Range	[0km,20km]	[0km,20km]
Number of nodes	18 nodes	98 nodes

TABLE 4. Results in the fixed network scenarios.

Approaches / Network / T(μs)	Mathematical model	Proposed LMI-MAPRA	Benchmark PSEA
18 node network	1037.68	1189	1479.1
98 node network	4862.5	5066.3	7274.3

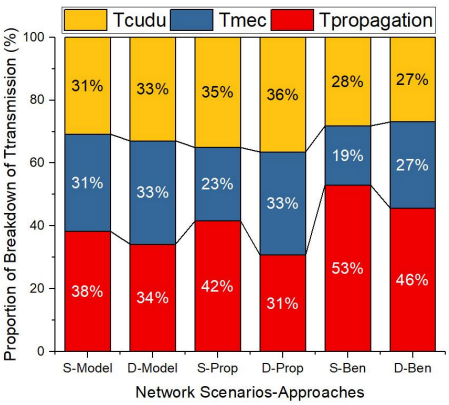

FIGURE 13. Proportion of breakdown of total transmission latency with approaches in both sparse and dense network scenarios.

5) APPLICATIONS IN THE FIXED NETWORK SCENARIOS

We simulated approaches for two fixed network scenarios of 18 nodes and 98 nodes, which are randomly located in an area of 20 × 20 km^2 as shown in Fig. 11 (a) and Fig. 12 (a). The simulation parameters are listed in Table 3. Simulation results of total transmission latencies in providing all services with different approaches are shown in Table 4. In the respective fixed networks of 18 node and 98 node, the proposed algorithm LMI-MAPRA reduces total transmission latencies by 19.6% and 30.4% as compared with the benchmark algorithm. In addition, the proposed algorithm differs from the accurate solution of the mathematical model by 14.6% and 4.2% in the respective fixed 18 and 98 node networks. The constructed optimal configuration topologies of MEC-enabled WDM-PON based FiWi Access Networks applied in the fixed networks are presented in Fig. 11 (b) and Fig. 12 (b). From simulation results as shown in Fig. 13, we observe

that the propagation latency occupies by 40.67% of the total transmission latency, and plays a dominant part among most of results obtained by different approaches in both the fixed 19 and 98 node networks.

V. CONCLUSION

In this paper, we developed a mathematical model for low-latency oriented network planning for WDM-PON based MEC-enabled Fiber Wireless Access Networks. To solve the mathematical model efficiently, we proposed a heuristic algorithm called LMI-MAPRA. We simulated this on different network scenarios to compare approaches on latency-minimized performances. The simulation results show that the proposed algorithm outperforms the benchmark algorithm in both sparse and dense networks, especially more significant in the dense network scenarios. In addition, the proposed algorithm LMI-MAPRA achieves near optimal results as compared with accurate solutions of the mathematical model in most of networks. The impacts of the number of MEC server and the number of CUDU-OLT on the comparison of different approaches are also evaluated. We also discuss the breakdown of total transmission latency.

REFERENCES

[1] B. P. Rimal, D. P. Van, and M. Maier, "Mobile edge computing empowered fiber-wireless access networks in the 5G era," *IEEE Commun. Mag.*, vol. 55, no. 2, pp. 192–200, Feb. 2017.
[2] Y. Ji, J. Zhang, Y. Xiao, and Z. Liu, "5G flexible optical transport networks with large-capacity, low-latency and high-efficiency," *China Commun.*, vol. 16, no. 5, pp. 19–23, May 2019.
[3] X. Wang, R. Gu, Y. Ji, and M. Kavehrad, "Hybrid services efficient provisioning over the network coding–enabled elastic optical networks," *Proc. SPIE*, vol. 56, no. 3, pp. 036101-1–036101-14, Mar. 2017.
[4] NTT DOCOMO. *DOCOMO 5G White Paper. Accessed:* 2018. [Online]. Available: https://www.nttdocomo.co.jp/english/corporate/technology/witepaper_5g/
[5] ARIB 2020 and Beyond Ad Hoc Group. *Mobile Communications Systems for 2020 and Beyond*. Accessed: 2018. [Online]. Available: http://www.arib.or.jp/english/20bah-wp100.pdf
[6] NGMN. (2014). *5G White Paper—Executive Version*. [Online]. Available: https://www.ngmn.org/fileadmin/user_upload/141222_NGMN-Executive_Version_of_the_5G_White_Paper_v1_0.pdfs
[7] Ericsson White Paper. *5G Radio Access—Capabilities and Technologies*. Accessed: 2018. [Online]. Available: https://www.ericsson.com/res/docs/whitepapers/wp-5g.pdf
[8] M. Satyanarayanan, R. Schuster, M. Ebling, G. Fettweis, H. Flinck, K. Joshi, and K. Sabnani, "An open ecosystem for mobile-cloud convergence," *IEEE Commun. Mag.*, vol. 53, no. 3, pp. 63–70, Mar. 2015.
[9] Y. C. Hu, M. Patel, D. Sabella, N. Sprecher, and V. Young, "Mobile-edge computing—A key technology towards 5G," ETSI, Sophia Antipolis, France, White Paper 11, Sep. 2015, pp. 1–16.
[10] J. Zhang, W. Xie, F. Yang, and Q. Bi, "Mobile edge computing and field trial results for 5G low latency scenario," *China Commun.*, vol. 13, no. 2, pp. 174–182, Feb. 2016.
[11] *Study on New Radio Access Technology; Radio Access Architecture and Interfaces*, document TR 38.801, Version 2.0.0, 3GPP, Mar. 2017.
[12] *Technical Specification Group Radio Access Network; Radio Frequency (RF) System Scenarios*, document 25.942, 3GPP, Jan. 2016.
[13] NGMN. (Oct. 2017). *5G End-to-End Architecture Framework*. [Online]. Available:https://www.ngmn.org/fileadmin/user_upload/170511_NGMN_E2EArchFramework_v0.6.5.pdf
[14] *5G White Paper V4.0 E: 5G Mobile/Multi-Access Edge Computing*, Next Gener. Mobile Netw. (NGMN) Alliance, Frankfurt, Germany, Nov. 2017.
[15] Y. Ji, J. Zhang, X. Wang, and H. Yu, "Towards converged, collaborative and co-automatic (3C) optical networks," *Sci. China Inf. Sci.*, vol. 61, no. 12, Dec. 2018, Art. no. 121301.
[16] J. Zhang, Y. Xiao, D. Song, L. Bai, and Y. Ji, "Joint wavelength, antenna, and radio resource block allocation for massive MIMO enabled beamforming in a TWDM-PON based fronthaul," *J. Lightw. Technol.*, vol. 37, no. 4, pp. 1396–1407, Feb. 15, 2019.
[17] J. Zhang, Y. Ji, H. Yu, X. Huang, and H. Li, "Experimental demonstration of fronthaul flexibility for enhanced CoMP service in 5G radio and optical access networks," *Opt. Express*, vol. 25, no. 18, pp. 21247–21258, Aug. 2017.
[18] Common Public Radio Interface (CPRI), "Common public radio interface (CPRI); interface specification," CPRI Specification V7.0, Common Public Radio Interface, Stockholm, Sweden, Tech. Rep. V7.0, 2015.
[19] A. Pizzinat, P. Chanclou, T. Diallo, and F. Saliou, "Things you should know about fronthaul," *J. Lightw. Technol.*, vol. 33, no. 5, pp. 1077–1083, Mar. 1, 2015.
[20] F. Ponzini, K. Kondepu, F. Giannone, P. Castoldi, and L. Valcarenghi, "Optical access network solutions for 5G fronthaul," in *Proc. 20th Int. Conf. Transp. Opt. Netw. (ICTON)*, Bucharest, Romania, 2018, pp. 1–5.
[21] S. Fili. (2012). *Wireless Backhaul Can Ease Transition to Fibre*. [Online]. Available: https://senzafili.com/
[22] X. Wang, R. Gu, and Y. Ji, "Ring-like reliable PON planning with physical constraints for a smart grid," *Opt. Fiber Technol.*, vol. 27, pp. 24–34, Jan. 2016.
[23] J. Li and G. Shen, "Cost minimization planning for greenfield passive optical networks," *IEEE/OSA J. Opt. Commun. Netw.*, vol. 1, no. 1, pp. 17–29, Jun. 2009.
[24] A. Agata and K. Nishimura, "Suboptimal PON network designing algorithm for minimizing deployment cost of optical fiber cables," in *Proc. 16th Int. Conf. Opt. Netw. Design Modelling (ONDM)*, Colchester, U.K., 2012, pp. 1–6.
[25] C. Ranaweera, E. Wong, A. Nirmalathas, C. Jayasundara, and C. Lim, "5G C-RAN with optical fronthaul: An analysis from a deployment perspective," *J. Lightw. Technol.*, vol. 36, no. 11, pp. 2059–2068, Jun. 1, 2017.
[26] X. Wang, L. Wang, C. Cavdar, M. Tornatore, G. B. Figueiredo, H. S. Chung, H. H. Lee, S. Park, and B. Mukherjee, "Handover reduction in virtualized cloud radio access networks using TWDM-PON fronthaul," *J. Opt. Commun. Netw.*, vol. 8, no. 12, pp. B124–B134, Dec. 2016.
[27] C. Ranaweera, C. Lim, A. Nirmalathas, C. Jayasundara, and E. Wong, "Cost-optimal placement and backhauling of small-cell networks," *J. Lightw. Technol.*, vol. 33, no. 18, pp. 3850–3857, Sep. 15, 2015.
[28] H. Chen, Y. Li, S. K. Bose, W. Shao, L. Xiang, Y. Ma, and G. Shen, "Cost-minimized design for TWDM-PONbased 5G mobile backhaul networks," *IEEE/OSA J. Opt. Commun. Netw.*, vol. 8, no. 11, pp. B1–B11, Nov. 2016.
[29] C. S. Ranaweera, P. P. Iannone, K. N. Oikonomou, K. C. Reichmann, and R. K. Sinha, "Cost optimization of fiber deployment for small cell backhaul," in *Proc. Opt. Fiber Commun. Conf., Nat. Fiber Optic Eng. Conf. (OFC/NFOEC)*, Anaheim, CA, USA, 2013, pp. 1–3.
[30] C. S. Ranaweera, P. P. Iannone, K. N. Oikonomou, K. C. Reichmann, and R. K. Sinha, "Design of cost-optimal passive optical networks for small cell backhaul using installed fibers [invited]," *IEEE/OSA J. Opt. Commun. Netw.*, vol. 5, no. 10, pp. A230–A239, Oct. 2013.
[31] C. Ranaweera, P. Monti, B. Skubic, M. Furdek, L. Wosinska, A. Nirmalathas, C. Lim, and E. Wong, "Optical X-haul options for 5G fixed wireless access: Which one to choose?" in *Proc. IEEE Conf. Comput. Commun. Workshops (IEEE INFOCOM WKSHPS)*, Honolulu, HI, USA, Apr. 2018, pp. 1–2.
[32] Y. Yu, C. Ranaweera, C. Lim, L. Guo, Y. Liu, A. Nirmalathas, and E. Wong, "Hybrid fiber-wireless network: An optimization framework for survivable deployment," *IEEE/OSA J. Opt. Commun. Netw.*, vol. 9, no. 6, pp. 466–478, Jun. 2017.
[33] R. I. Tinini, L. C. M. Reis, D. M. Batista, G. B. Figueiredo, M. Tornatore, and B. Mukherjee, "Optimal placement of virtualized BBU processing in hybrid cloud-fog RAN over TWDM-PON," in *Proc. IEEE Global Commun. Conf. (GLOBECOM)*, Singapore, Dec. 2017, pp. 1–6.
[34] S. Sarkar, H. H. Yen, S. Dixit, and B. Mukherjee, "Hybrid wireless-optical broadband access network (WOBAN): Network planning and setup," *IEEE J. Sel. Areas Commun.*, vol. 26, no. 6, pp. 12–21, Aug. 2008.
[35] J. Zhang, Y. Ji, J. Zhang, R. Gu, Y. Zhao, S. Liu, K. Xu, M. Song, H. Li, and X. Wang, "Baseband unit cloud interconnection enabled by flexible grid optical networks with software defined elasticity," *IEEE Commun. Mag.*, vol. 53, no. 9, pp. 90–98, Sep. 2015.
[36] J. Zhang, Y. Ji, S. Jia, H. Li, X. Yu, and X. Wang, "Reconfigurable optical mobile fronthaul networks for coordinated multipoint transmission and reception in 5G," *IEEE/OSA J. Opt. Commun. Netw.*, vol. 9, no. 6, pp. 489–497, Jun. 2017.

[37] A. Reznik, L. M. C. Murillo, Y. Fang, W. Featherstone, M. Filippou, F. Fontes, F. Giust, Q. Huang, A. Li, C. Turyagyenda, C. Wehner, and Z. Zheng, "Cloud RAN and MEC: A perfect pairing," ETSI, Sophia Antipolis, France, ETSI White Papers 23, 2018. [Online]. Available: https://www.etsi.org/images/files/ETSIWhitePapers/etsi_wp23_MEC_andCRAN_ed1_FINAL.pdf

[38] X. Chen, L. Jiao, W. Li, and X. Fu, "Efficient multi-user computation offloading for mobile-edge cloud computing," *IEEE/ACM Trans. Netw.*, vol. 24, no. 5, pp. 2795–2808, Oct. 2016.

[39] L. Mo, W. Cheng, and L. M. Contreras, "ZTE 5G transport solution and joint field trials with global operators," in *Proc. Opt. Fiber Commun. Conf. (OFC)*, San Diego, CA, USA, 2019, pp. 1–3, Paper M1G.2.

[40] T. Soyata, R. Muraleedharan, C. Funai, M. Kwon, and W. Heinzelman, "Cloud-vision: Real-time face recognition using a mobile-cloudlet-cloud acceleration architecture," in *Proc. IEEE Symp. Comput. Commun. (ISCC)*, Cappadocia, Turkey, Jul. 2012, pp. 59–66.

[41] *Physical Channels and Modulation*, document 3GPP TS 38.211, 2017. [Online]. Available: http://www.3gpp.org/ftp/Specs/archive/38_series/38.211/

[42] J. F. Myoupo and A. C. Fabret, "A modular systolic linearization of the Warshall-Floyd algorithm," *IEEE Trans. Parallel Distrib. Syst.*, vol. 7, no. 5, pp. 449–455, May 1996.

XIN WANG received the Ph.D. degree from the State Key Laboratory of Information Photonics and Optical Communications, Beijing University of Posts and Telecommunications (BUPT), China. She was a Visiting Ph.D. Student with Pennsylvania State University, State College, PA, USA. She currently holds the postdoctoral position at BUPT. Her research interests include converged optical and wireless networks and machine learning-based network optimization.

YUEFENG JI received the Ph.D. degree from the Beijing University of Posts and Telecommunications, China, where he is currently a Professor and the Deputy Director of the State Key Laboratory of Information Photonics and Optical Communications. His research interests include broadband communication networks and optical communications, with an emphasis on key theory, realization of technology, and applications. He is a Fellow of CIC, CIE, and IET.

JIAWEI ZHANG received the Ph.D. degree from the State Key Laboratory of Information Photonics and Optical Communications, Beijing University of Posts and Telecommunications (BUPT), China. He was a joint supervised Ph.D. with the University of California at Davis, USA. He is currently an Associate Professor with BUPT. His current research interests include 5G RAN transport networks, network function virtualization, software-defined radio, and optical access networks.

LIN BAI received the M.S. degree from the Beijing University of Posts and Telecommunications (BUPT), where she is currently a Professor. Her research interests include management information service and communication networks.

MIN ZHANG received the Ph.D. degree in optical communications from the Beijing University of Posts and Telecommunications (BUPT), China, where he is currently a Professor, the Deputy Director of the State Key Laboratory of Information Photonics and Optical Communications, and the Deputy Dean of the School of Optoelectronic Information. He holds 45 China patents. He has authored or coauthored over 300 technical papers in international journals and conferences and 12 books in the area of optical communications. His main research interests include optical communication systems and networks, optical signal processing, and optical wireless communications.